

A sampling scheme for estimating the prevalence of a pandemic

Ze Liu¹, Siyu Yi¹, Jianghu (James) Dong², Min-Qian Liu¹ and Yongdao Zhou ^{*1}

¹School of Statistics and Data science, LPMC & KLMDASR, NanKai University, Tianjin, China

²Department of Biostatistics, College of Public Health, University of Nebraska Medical Center, Omaha,
Nebraska, U.S.A.

Abstract

The spread of COVID-19 makes it essential to investigate its prevalence. In such investigation research, as far as we know, the widely-used sampling methods didn't use the information sufficiently about the numbers of the previously diagnosed cases, which provides a priori information about the true numbers of infections. This motivates us to develop a new, two-stage sampling method in this paper, which utilises the information about the distributions of both population and diagnosed cases, to investigate the prevalence more efficiently. The global likelihood sampling, a robust and efficient sampler to draw samples from any probability density function, is used in our sampling strategy, and thus, our new method can automatically adapt to the complicated distributions of population and cases.

Moreover, the corresponding estimating method is simple, which facilitates the practical

*ydzhou@nankai.edu.cn

implementation. Some recommendations for practical implementation are given. Finally, several simulations and a practical example verified its efficiency.

Keywords: COVID-19, global likelihood sampling, sampling survey.

MSC2010: 62D05, 62P10, 65C05.

1. Introduction

COVID-19 broke out at the end of 2019 and was declared a global pandemic by WHO (2020). All countries around the world were severely affected, especially the United States of America (USA), where the numbers of confirmed cases and deaths increased rapidly from March 2020 to April 2021 (Centers for Disease Control and Prevention 2020). It is essential for the government and health institutions to monitor COVID-19 and control the pandemic by making practical and reasonable plans.

Since some people infected by SARS-CoV-2 are asymptomatic (Sakurai et al. 2020), one main difficulty with the pandemic is that the cumulative number of diagnosed cases cannot represent the number of infections. Many countries have made efforts to investigate the prevalence of COVID-19 (Anand et al. 2020; Stringhini et al. 2020; Pollán et al. 2020; Xu et al. 2020; Havers et al. 2020; Rosenberg et al. 2020; Sood et al. 2020; Ward et al. 2021); however, many of these investigations (Stringhini et al. 2020; Xu et al. 2020; Havers et al. 2020; Sood et al. 2020) only focused on one or several hotspot(s) instead of the whole country. In addition, when investigating the prevalence nationwide, restricted by the costs, only a small part of the whole population can be investigated, especially when the country has a broad territory area. Therefore, it is important to develop some appropriate sampling strategies. The use of convenience samples (Stringhini et al. 2020; Xu et al. 2020; Havers et al. 2020; Rosenberg et al. 2020; Kissler et al. 2020) is not proper because they are prone to the selection bias, and thus, problematic. Some

other literature work (Leong et al. 2021; Parenteau et al. 2021; Knudsen et al. 2021; Tian et al. 2021; Sartorius et al. 2021) drew samples from some representative databases — for example, the medical insurance databases. This strategy can reduce the cost of the survey, but the representativeness of such samples depends on the representativeness of the database. Another popular sampling strategy used in the investigations of prevalence is the multi-stage stratified sampling, or some variants of it. Some recent studies (Jia et al. 2020; Pollán et al. 2020; Ward et al. 2021; Nagashima et al. 2021; Ssentongo et al. 2021; Horton-French et al. 2021; Mulenga et al. 2021; Li et al. 2021) have used these kinds of sampling methods. Compared with the simple random sampling, the variance of the estimator obtained by the stratified sampling is usually smaller. However, this method depends heavily on the construction of the strata in which the inter-homogeneity is required, and sometimes a well-designed stratified sampling strategy may lead to a very complex analysis procedure.

Intuitively, the distribution of the number of cumulative cases provides priori information about the true situation of infections, and, therefore, can help with the sampling survey to improve the efficiency. However, none of the above research utilised this priori information sufficiently. In this paper, we propose a new sampling strategy for estimating the total number of infections nationwide. The main feature of this method is that it can flexibly and efficiently utilise the information about the distributions of both population and diagnosed cases. Compared with the stratified multi-stage sampling, our method is more flexible to adapt to various complicated distributions of population and cases. The implementation and the corresponding estimating methods of this sampling strategy are also easier. There are two stages in the sampling strategy: first, determining the sampling positions according to some probability density, and then sampling from these positions. The main focus of this paper is on the first

stage, in which the probability density may be multimodal and complicated. In this situation, some well-known methods to sample from a general probability density function, including the Markov Chain Monte Carlo (MCMC) method, e.g. Metropolis-Hastings (MH) algorithm (Hastings 1970), and the sampling/importance resampling (SIR) method (Rubin 1987), as well as its variants (Pérez et al. 2005; Ning and Tao 2018), may have a bad performance. The reason is that those methods can't adapt to various kinds of sampling densities (the MCMC method is easy to get stuck at some peak of the density function when the sampling density is multimodal, and the performance of the SIR depends heavily on the choice of the proposal distribution and the quality of the initial samples from the proposal distribution). To overcome these problems, Wang et al. (2015) proposed a new method, called the global likelihood sampling (GLS), which is also used in the first stage of our proposed sampling strategy. As for the second stage, any advanced sampling strategy can be used, but for simplicity, we only consider the simple random sampling method in this paper.

The rest of this paper is organised as follows. In Section 2, we describe the problem and propose the basic approach. The GLS algorithm is also described in this section. In Section 3, the optimal settings of our sampling strategy are derived. The complete sampling strategy and the corresponding estimating method are given in Section 4, as well as some suggestions for practical implementation. Some numerical simulations are conducted in Section 5, in order to find the robust setting of a parameter in our method, and to show the efficiency of our method. To further explain our method, a practical example is presented in Section 6. Finally, Section 7 concludes this paper. Some additional remarks, details and simulations are provided in the supplementary material.

2. Preliminaries

2.1. Basic Approach

Suppose a pandemic is spreading over a region $\mathcal{R} \subseteq \mathbb{R}^2$, and we want to know its total prevalence over the region \mathcal{R} . The total population of this region, the cumulative number of diagnosed cases, and the cumulative number of real infections are denoted by N_P , N_D and N_I , respectively. The corresponding densities of population, cases and infections in \mathcal{R} are f_P , f_D and f_I , respectively, and

$$\int_{\mathcal{R}} f_i(x) dx = N_i$$

with i being P, D and I. The information about the population, N_P and f_P , and that about the diagnosed cases, N_D and f_D , are usually known, but the information about the real infections, N_I and f_I , is hard to get, which is just what we are interested in. Since the total prevalence is N_I/N_P , estimating the total prevalence is equivalent to estimating the total number of infections N_I . Therefore, for convenience, our goal is to estimate N_I by a sampling survey.

Denote $\mathcal{L}_k := \{1, \dots, k\}$ for any $k \in \mathbb{N}^+$ where \mathbb{N}^+ is the set of all positive integers. Since N_I is the integral of f_I on \mathcal{R} , a popular way to approximate N_I is the Monte Carlo method: let φ be a probability density function on \mathcal{R} and ξ_1, \dots, ξ_r be r independent and identically distributed (i.i.d.) samples from φ , then the sample mean $r^{-1} \sum_{i=1}^r f_I(\xi_i) / \varphi(\xi_i)$ is an unbiased estimator of N_I . Hereafter, we call φ the sampling density and call ξ_1, \dots, ξ_r the sampling positions. Since f_I is unknown, we have to estimate the values of f_I at ξ_1, \dots, ξ_r . Therefore, our sampling survey consists of two stages: first, determining the sampling positions ξ_1, \dots, ξ_r ; second, selecting the samples, i.e., the people who will receive the tests, at each sampling position to estimate the values of f_I there. The main focus of this paper is on the first stage, and the simple random

sampling is adopted in the second stage. Other advanced sampling methods can also be used in the second stage, which is problem-dependent.

Denote the local prevalence function over \mathcal{R} by $\rho_I := f_I/f_P$. Let x be an arbitrary fixed position in the region \mathcal{R} , and n_x be the fixed sample size at x . Then, n_x people from the sampling position x are tested. For each $i \in \mathcal{L}_{n_x}$, let $\tau_i = 1$ if the i -th person was infected, and $\tau_i = 0$ otherwise. Intuitively, one person's possibility of infection is associated with the infection status of others in that person's household/neighbourhood/community. This correlation can be characterised by the local prevalence function ρ_I . Moreover, n_x is usually very small compared to the population around the position x . Hence, we can consider, approximately, that $\tau_1, \dots, \tau_{n_x} \stackrel{\text{i.i.d.}}{\sim} \text{Bi}(1, \rho_I(x))$, where Bi represents the binomial distribution. An unbiased estimator of $f_I(x)$ is

$$\hat{f}_I(x) := f_P(x) \cdot \frac{1}{n_x} \sum_{i=1}^{n_x} \tau_i, \quad (1)$$

with its variance being

$$\text{Var}[\hat{f}_I(x)] = \frac{f_I(x) [f_P(x) - f_I(x)]}{n_x}. \quad (2)$$

Hence, in order to get the estimations of $f_I(\xi_1), \dots, f_I(\xi_r)$, we have to determine the sample sizes at ξ_1, \dots, ξ_r . Suppose the expected total sample size is n , and v is a positive function on \mathcal{R} such that

$$\int_{\mathcal{R}} v(x) \varphi(x) dx = \frac{n}{r}. \quad (3)$$

When the position $x \in \mathcal{R}$ is selected in the first stage, the sample size at x will be $v(x)$, approximately. Hereafter, we call v the allocation function of the sample sizes. Combining the results of the two stages, we obtain an unbiased estimator of the total number of infections N_I ,

$$\hat{N}_I := \frac{1}{r} \sum_{i=1}^r \frac{\hat{f}_I(\xi_i)}{\varphi(\xi_i)}. \quad (4)$$

The unbiasedness of \hat{N}_I can be easily verified using the law of total expectation as follows:

$$\mathbb{E}(\hat{N}_I) = \mathbb{E} \left[\frac{\hat{f}_I(\xi_1)}{\varphi(\xi_1)} \right] = \mathbb{E} \left\{ \mathbb{E} \left[\frac{\hat{f}_I(\xi_1)}{\varphi(\xi_1)} \middle| \xi_1 \right] \right\} = \mathbb{E} \left[\frac{f_I(\xi_1)}{\varphi(\xi_1)} \right] = \int_{\mathcal{R}} \frac{f_I(x)}{\varphi(x)} \cdot \varphi(x) dx = N_I. \quad (5)$$

Similarly, we can obtain its variance

$$\text{Var}(\hat{N}_I) = \frac{1}{r} \left\{ \text{Var} \left[\frac{f_I(\xi_1)}{\varphi(\xi_1)} \right] + \mathbb{E} \left[\frac{f_I(\xi_1) [f_P(\xi_1) - f_I(\xi_1)]}{v(\xi_1) [\varphi(\xi_1)]^2} \right] \right\} = \frac{1}{r} \cdot [v_0(\hat{N}_I) + v_1(\hat{N}_I)]. \quad (6)$$

By the central limit theorem,

$$\frac{\hat{N}_I - N_I}{\sqrt{\text{Var}(\hat{N}_I)}} \xrightarrow{d} \text{N}(0, 1) \quad \text{as } r \rightarrow +\infty, \quad (7)$$

where ‘ \xrightarrow{d} ’ means the convergence in distribution, and $\text{N}(0, 1)$ is the standard normal distribution. Based on (7), we can construct the approximate confidence intervals for N_I when r is large enough. It is hinted by the Supplementary Material that the least r required for well approximating this asymptotic distribution can be very small, which is completely achievable in practice.

2.2. Global Likelihood Sampling

The sampling strategy introduced in Section 2.1 involves sampling from a bi-variate probability density function φ . Since the form of φ can be various, multimodal and complicated, the extraction of ξ_1, \dots, ξ_r is not easy, and some well-known methods, e.g. MCMC and SIR, may be not suitable. Instead, we adopt the GLS algorithm, which applies to the multimodal and complicated cases, to generate the r sampling positions. Detailed discussion can refer to Zhou et al. (2021). Algorithm 1 describes the GLS method for generating i.i.d. samples ξ_1, \dots, ξ_r from φ . The GLS used here is simplified compared to the original one in Wang et al. (2015).

The performance of Algorithm 1 depends on the uniformity of D . Intuitively, the better the uniformity of D , the better $\mathcal{P}^{(i)}$ approximates φ for each $i \in \mathcal{L}_r$, and, therefore, the better the

Algorithm 1: GLS algorithm

Let the smallest rectangle containing \mathcal{R} be $\bar{\mathcal{R}} \subseteq \mathbb{R}^2$; without loss of generality, suppose

$$\bar{\mathcal{R}} = [0, 1]^2.$$

Input: the kernel of the sampling density: \check{f}_I ; a uniform design on $\bar{\mathcal{R}}$:

$$D = \{q_j : j \in \mathcal{L}_M\}.$$

Step 1. Loop. Repeat Steps 2 to 4 for $i = 1, \dots, r$.

Step 2. Random shift. Generate $\delta^{(i)} \sim U(\bar{\mathcal{R}})$ and let $D^{(i)} = \{q_j \oplus \delta^{(i)} : j \in \mathcal{L}_M\}$

$= D \oplus \delta^{(i)}$, where the operator \oplus means the addition modulo 1, i.e. adding first and then taking the fractional part for each component.

Step 3. Likelihood. For each $x \in D^{(i)}$, let $w^{(i)}(x) = \check{f}_I(x) / \sum_{y \in D^{(i)}} \check{f}_I(y)$, where $\check{f}_I(x) = 0$ for $x \in \bar{\mathcal{R}} \setminus \mathcal{R}$. Then $\mathcal{P}^{(i)} = \{(x, w^{(i)}(x)) : x \in D^{(i)}\}$ is a multinomial distribution on $D^{(i)}$.

Step 4. Sampling. Generate ξ_i in $D^{(i)}$ from the multinomial distribution $\mathcal{P}^{(i)}$.

Output: r i.i.d. samples from φ : ξ_1, \dots, ξ_r .

empirical distribution of ξ_1, \dots, ξ_r approximates φ . There are some additional remarks about the region $\bar{\mathcal{R}}$ and the uniform design D in Algorithm 1 in the Supplementary Material.

3. Optimal Settings of the Parameters

In the two-stage sampling strategy introduced in Section 2.1, there are three adjustable parameters: the sampling density φ , the allocation function of the sample sizes ν , and the number of sampling positions r . From (5), (6) and (7), these three parameters do not affect the unbiasedness of \hat{N}_I , but do affect its variance and distribution. In this section, we discuss the optimal settings of these parameters, where ‘optimal’ means to minimise the variance of \hat{N}_I .

First, we consider ν , since it only affects the term $\nu_1(\hat{N}_I)$ in (6). By the Lagrange multiplier

method, we can find that under the constraint (3), $v_1(\hat{N}_I)$ is minimised when for any $x \in \mathcal{R}$,

$$v(x) = \frac{n}{r \int_{\mathcal{R}} \tilde{f}(y) dy} \cdot \frac{\tilde{f}(x)}{\varphi(x)}, \quad (8)$$

where $\tilde{f} := \sqrt{f_I(f_P - f_I)}$. The minimum of $v_1(\hat{N}_I)/r$ is $[\int_{\mathcal{R}} \tilde{f}(x) dx]^2/n$, which is independent of the settings of φ and r . Then note that $v_0(\hat{N}_I) = 0$ when $\varphi \propto f_I$, hence no matter what r is, when $\varphi \propto f_I$ and v is set as (8), $\text{Var}(\hat{N}_I)$ is minimised with the minimum being

$$\frac{1}{n} \left[\int_{\mathcal{R}} \tilde{f}(x) dx \right]^2. \quad (9)$$

However, the above optimal settings of φ and v cannot be achieved in practice because those optimal settings depend on f_I , which is unknown, and is just what we want to estimate. Instead, we need to find the nearly optimal settings of φ and v . We first consider the following mechanism to determine an initial rough estimate of f_I . Without any extra knowledge, the only information about f_I is $0 \leq f_D \leq f_I \leq f_P$, which implies that there exists a function γ from \mathcal{R} to $[0, 1]$ such that $f_I = \gamma \cdot f_P + (1 - \gamma) \cdot f_D$. It is impossible to know the form of γ unless some extra information is given. A simple but reasonable way is to choose a proper constant $\check{\gamma} \in [0, 1]$ and take

$$\check{f}_I := \check{\gamma} \cdot f_P + (1 - \check{\gamma}) \cdot f_D \quad (10)$$

as an initial rough estimate of f_I . This estimation combines the information of both f_P and f_D , which can make our method efficient. With the estimator \check{f}_I , the nearly optimal setting of φ is $\check{f}_I / [\check{\gamma} \cdot N_P + (1 - \check{\gamma}) \cdot N_D]$. As for v , we can use $\check{\tilde{f}} := \sqrt{\check{f}_I(f_P - \check{f}_I)}$ to estimate \tilde{f} in (8), but there remains an integral $\int_{\mathcal{R}} \check{\tilde{f}}(y) dy$ to approximate. Since the form of $\check{\tilde{f}}$ is generally complicated, it is appropriate to approximate this integral using the Monte Carlo method. In fact, since the r positions ξ_1, \dots, ξ_r are i.i.d. samples from φ , the sample mean

$$\frac{1}{r} \cdot \sum_{i=1}^r \frac{\check{\tilde{f}}(\xi_i)}{\varphi(\xi_i)}$$

is an unbiased estimator of the integral $\int_{\mathcal{R}} \tilde{f}(y) dy$. Therefore, for each $i \in \mathcal{Z}_r$, the nearly optimal sample size at the sampling position ξ_i , which is an approximation of the exact optimal $v(\xi_i)$, is

$$n_{\xi_i} := \frac{\check{f}(\xi_i)/\varphi(\xi_i)}{\sum_{j=1}^r \check{f}(\xi_j)/\varphi(\xi_j)} \cdot n.$$

With the nearly optimal setting of φ , it is simplified to

$$n_{\xi_i} = \frac{\sqrt{[f_P(\xi_i) - \check{f}_I(\xi_i)] / \check{f}_I(\xi_i)}}{\sum_{j=1}^r \sqrt{[f_P(\xi_j) - \check{f}_I(\xi_j)] / \check{f}_I(\xi_j)}} \cdot n. \quad (11)$$

This allocation method of sample sizes has the benefit that the total sample size is exactly n , which meets the requirement in most practical situations.

Next, we consider the number of sampling positions r . From (3) and (8), v is approximately proportional to $1/r$, thus $v_1(\hat{N}_I)/r$ in (6) is always approximately independent of r , and a large r can reduce $\text{Var}(\hat{N}_I)$ by reducing $v_0(\hat{N}_I)/r$. Therefore, r should be large in order to reduce the variance when φ is not exactly proportional to f_I , as long as n_{ξ_i} is not too small to estimate the value of f_I at ξ_i for each $i \in \mathcal{Z}_r$. By (7), a large r also helps to obtain a good approximate distribution of \hat{N}_I . The numerical simulations in the Supplementary Material show that larger r can notably reduce the variance and improve the coverage rate of the confidence interval. Note that in practice, larger r may also increase the cost and the difficulty of the sampling survey, since more positions have to be sampled. These results are consistent with the classical sampling theory (Cochran 1977).

In addition, the costs at different sampling positions may be different in practice, which can be quantified by a cost function c over \mathcal{R} . Then our goal is to find the appropriate parameters which can minimise both of $\text{Var}(\hat{N}_I)$ and the total cost. For example, the weighted sum of $\text{Var}(\hat{N}_I)$ and the total cost can be used as an optimality criterion, i.e., $\text{Var}(\hat{N}_I) +$

$\gamma_c \int_{\mathcal{R}} c(x)v(x)\varphi(x) dx$ where $\gamma_c \in [0, +\infty)$ reflects the importance of the total cost. For such cases, an analysis similar to the above can be performed, but it may be difficult to derive the explicit expressions. Instead, the numerical optimisation algorithms can be considered to solve this problem, which is beyond the scope of this paper.

4. Sampling and Estimating

Based on the discussion about the nearly optimal settings of the parameters in Section 3, we show the complete sampling strategy and the estimating method in this section. Some suggestions for the practical implementation are also given.

The details of the two-stage sampling strategy are described in Algorithm 2, which combines the basic approach in Section 2.1 with the GLS algorithm in Section 2.2.

Algorithm 2: Two-stage sampling strategy

Input: a proper constant in $[0, 1]$ to give a rough estimator of f_I : $\check{\gamma}$; the uniform design used in Algorithm 1: D ; the total sample size: n ; the number of sampling positions: r .

Step 1. Rough estimate. Obtain \check{f}_I , an initial rough estimator of f_I , by (10). The kernel of the sampling density φ is set to be \check{f}_I .

Step 2. Sampling positions. Generate r i.i.d. sampling positions ξ_1, \dots, ξ_r in \mathcal{R} from the sampling density φ by the GLS in Algorithm 1.

Step 3. Allocation of sample sizes. For each $i \in \mathcal{L}_r$, calculate $\text{round}(n_{\xi_i})$, the sample size at the sampling position ξ_i , where n_{ξ_i} is calculated by (11) and ‘round’ is the function rounding a real number into the nearest integer.

Step 4. Test. For each $i \in \mathcal{L}_r$, select $\text{round}(n_{\xi_i})$ people at position ξ_i by the simple random sampling and then implement tests on them.

Next, we give some remarks about Algorithm 2 as follows.

1. About n . In practice, the n is usually determined by both the requirement of precision and the restriction of costs, thus $\text{Var}(\hat{N}_I)$ should be roughly estimated before the implementation of the sampling strategy. This can be done by using (9), which can be approximated by

$$\frac{1}{n} \left[\frac{\mathbf{m}(\mathcal{R})}{M} \sum_{x \in D} \check{f}(x) \right]^2$$

where $\mathbf{m}(\mathcal{R})$ is the area of \mathcal{R} . The n should be set such that the above estimator of $\text{Var}(\hat{N}_I)$ is smaller than some pre-defined threshold about the precision.

2. About n_{ξ_i} . As mentioned in Section 3, r should be as large as possible, provided that the cost will not exceed the budget, and no n_{ξ_i} is too small to estimate $f_I(\xi_i)$. An additional way to avoid small n_{ξ_i} is to modify the calculation method of the sample sizes at those sampling positions, i.e., the n_{ξ_i} in Step 3 of Algorithm 2 as

$$n_{\xi_i} := \frac{\sqrt{[f_P(\xi_i) - \check{f}_I(\xi_i)] / \check{f}_I(\xi_i)}}{\sum_{j=1}^r \sqrt{[f_P(\xi_j) - \check{f}_I(\xi_j)] / \check{f}_I(\xi_j)}} \cdot (1 - \eta)n + \frac{1}{r} \cdot \eta n, \quad (12)$$

where $\eta \in [0, 1]$ is a properly chosen constant. Since the allocation method of sample sizes in (11) is nearly optimal, η in (12) should not be too large. The proper setting of η should make the minimum sample size among those sampling positions just achieve some pre-defined threshold. Further, if n_{ξ_i} is not very small compared to the population around the sampling position ξ_i , finite population corrections (Cochran 1977; Lohr 2019) should be applied. For such case, expression (2) becomes

$$\text{Var}[\hat{f}_I(x)] = [1 - \rho_S(x)] \cdot \frac{f_I(x)[f_P(x) - f_I(x)]}{n_x}$$

where $\rho_S(x)$ refers to the sampling fraction at $x \in \mathcal{R}$, and $v_1(\hat{N}_I)$ in (6) becomes

$$E \left\{ [1 - \rho_S(\xi_1)] \cdot \frac{f_I(\xi_1) [f_P(\xi_1) - f_I(\xi_1)]}{v(\xi_1) [\varphi(\xi_1)]^2} \right\}.$$

3. About the sampling survey at each sampling position. For each $i \in \mathcal{Z}_r$, in practice, the n_{ξ_i} samples come from not exactly ξ_i , but a neighbourhood of ξ_i . For convenience, this neighbourhood can be chosen as some small district, like a city, village, or community, containing ξ_i or just close to ξ_i . It won't affect the property of this sampling strategy as long as the diameter of the neighbourhood is negligible compared to the whole region \mathcal{R} . For example, the samples at each ξ_i can be drawn from the people whose current residences are within the circle centred at ξ_i with radius 10km. Some other popular sampling methods, such as the stratified sampling, cluster sampling, multi-stage sampling and other techniques (Lohr 2019), can be used to estimate $f_I(\xi_i)$ more efficiently. The corresponding results can be obtained similarly with suitable modifications.

In addition, it is difficult to theoretically optimise the setting of $\check{\gamma}$, but the numerical studies will give some recommendations in Section 5.1.

Our main purpose is to estimate the cumulative total number of infections N_I . With the testing results obtained by the above sampling strategy, we can estimate N_I by using (1) and (4). The variance of the estimator can also be estimated by (6), and then an approximate confidence interval (CI) can be constructed according to (7). This estimating procedure is described in detail as follows.

Step 1. For $i = 1, \dots, r$, calculate $\hat{f}_I(\xi_i)$ by (1) using the testing results at the sampling position ξ_i , and calculate $\varphi(\xi_i)$ where $\varphi = \check{f}_I / [\check{\gamma} \cdot N_P + (1 - \check{\gamma}) \cdot N_D]$.

Step 2. Obtain the point estimator \hat{N}_I of the total number of infections N_I according to (4).

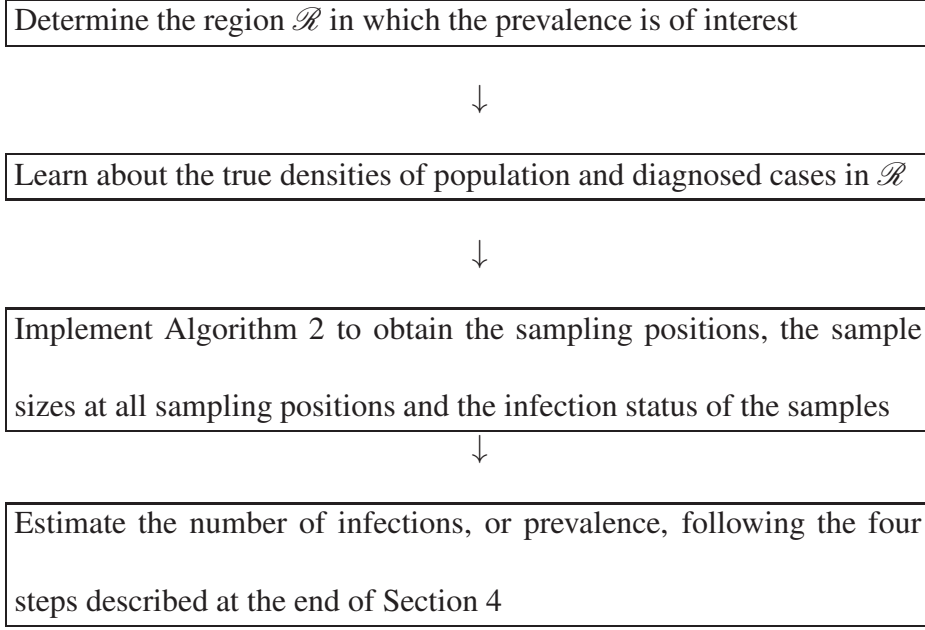


Figure 1. The complete procedure for implementing the proposed sampling method.

Step 3. According to (6), let

$$\begin{aligned}
 \hat{v}_0(\hat{N}_I) &:= \frac{1}{r-1} \sum_{i=1}^r \left[\frac{\hat{f}_I(\xi_i)}{\varphi(\xi_i)} - \hat{N}_I \right]^2, \\
 \hat{v}_1(\hat{N}_I) &:= \frac{1}{r} \sum_{i=1}^r [1 - \rho_S(\xi_i)] \cdot \frac{\hat{f}_I(\xi_i) [f_P(\xi_i) - \hat{f}_I(\xi_i)]}{n_{\xi_i} [\varphi(\xi_i)]^2}, \\
 \hat{v}(\hat{N}_I) &:= \frac{1}{r} \cdot [\hat{v}_0(\hat{N}_I) + \hat{v}_1(\hat{N}_I)],
 \end{aligned} \tag{13}$$

then $\hat{v}(\hat{N}_I)$ is an estimator of $\text{Var}(\hat{N}_I)$.

Step 4. According to (7), an approximate $1 - \alpha$ CI of N_I is $[\hat{N}_I - z_{\alpha/2} \sqrt{\hat{v}(\hat{N}_I)}, \hat{N}_I + z_{\alpha/2} \sqrt{\hat{v}(\hat{N}_I)}]$, where $z_{\alpha/2}$ is the upper $\alpha/2$ -quantile of $N(0, 1)$.

Hence, by the two-stage sampling strategy and the estimating method above, we can obtain the estimator of N_I , its estimated variance and approximate CI. The complete procedure is summarised in Figure 1. In the next two sections, we will show some numerical simulations and a practical example to verify the validity of our proposed sampling strategy.

5. Numerical Simulation

In Section 3 and Section 4, we discussed how to set the parameters in the two-stage sampling strategy, except for the coefficient $\check{\gamma}$ in (10). In this section, we first give a robust setting for $\check{\gamma}$ in the minimax sense through some numerical simulations, when there is little information about the underlying true f_I . Then we compare our proposed sampling strategy with some other popular methods to verify the efficiency of our method.

5.1. Robust Setting of $\check{\gamma}$

In the oracle situation, when the exact optimal settings of v and φ discussed in Section 3 can be achieved, the variance of \hat{N}_I is minimised, denoted by $\text{Var}(\hat{N}_I | \varphi \propto f_I)$. On the other hand, when we do not know the true f_I and have to use the initial rough estimator (10) to determine the sample sizes and the sampling density, the variance of \hat{N}_I , denoted by $\text{Var}(\hat{N}_I | \varphi \propto \check{f}_I)$, depends on the quality of \check{f}_I , and thus depends on $\check{\gamma}$. Therefore, in order to measure the performance of different settings of \check{f}_I or $\check{\gamma}$, we define the standardised standard deviation (SSD) as

$$\text{SSD}(\check{\gamma}) = \text{SSD}(\check{f}_I) := \sqrt{\frac{\text{Var}(\hat{N}_I | \varphi \propto \check{f}_I)}{\text{Var}(\hat{N}_I | \varphi \propto f_I)}}.$$

Our goal is to find the setting of $\check{\gamma}$ such that the maximum of SSD over all possible true f_I 's is minimised at that $\check{\gamma}$.

In the simulations, the region $\mathcal{R} = [0, 1]^2$ is the unit square and it is divided into four equal-sized sub-squares. Let the populations in them be 20, 40, 60 and 80, multiplied by 1×10^4 respectively, and the numbers of cases in them be 6, 8, 4 and 2, multiplied by 1×10^4 respectively. Dividing those numbers by $1/4$ will obtain the corresponding densities in the sub-squares. Fol-

lowing is the corresponding graph.

$$\text{Populations } (\times 10^4): \begin{array}{|c|c|} \hline 20 & 40 \\ \hline 60 & 80 \\ \hline \end{array}, \quad \text{Numbers of cases } (\times 10^4): \begin{array}{|c|c|} \hline 6 & 8 \\ \hline 4 & 2 \\ \hline \end{array}.$$

The total population $N_P = 200 \times 10^4$ and the total number of cases $N_D = 20 \times 10^4$. We set the size of the uniform design used in the GLS algorithm $M = 210$, the total sample size $n = 1 \times 10^4$ and the number of sampling positions $r = 50$. In different groups of simulations, the settings of f_I will be different. For each setting of f_I and $\check{\gamma}$, $\text{Var}(\hat{N}_I)$ is calculated using the sample variance of \hat{N}_I over 200 independent simulations.

In the first series of simulations, Series E, assume the true density of the infections f_I is a convex combination of f_P and f_D , i.e. $f_I = \gamma f_P + (1 - \gamma) f_D$, where $\gamma \in [0, 1]$ is a constant. Series E contains three groups of simulations, E1 to E3, whose settings are shown in Table 1, and the corresponding results are given in Figure 2. For each setting of f_I (or γ) in Group E1, the coefficient $\check{\gamma}$ takes 19 different values, and the corresponding 19 values of $\text{SSD}(\check{\gamma})$ form a black curve in Figure 2(a). The robust setting of $\check{\gamma}$ is the one that minimises the maximum SSD among the 19 settings of f_I , i.e., the one that minimises the red bold curve in Figure 2(a), which is marked out by a red circle. The other two subfigures are obtained similarly. The three subfigures in Figure 2 present a similar phenomenon that in the domain of γ , the maximum SSD is large when $\check{\gamma}$ is close to the bounds of the domain, while the maximum SSD is minimised when $\check{\gamma}$ is neither too large nor too small. Therefore, Figure 2 indicates that when a possible range of the true value of γ is available, the mid-point of that range may be a robust setting of $\check{\gamma}$.

In order to verify this conclusion, another series of simulations, Series R, is conducted. In this series, the true density of the infections is more complex than that in Series E. For each $i \in \mathcal{L}_4$, the density of infections in the i -th sub-square is $f_{I,i} = \gamma_i f_{P,i} + (1 - \gamma_i) f_{D,i}$, where

Table 1. Settings of f_I and $\check{\gamma}$ in the simulations in Series E.

	Group E1	Group E2	Group E3
γ	$\{0.05, 0.1, \dots, 0.9, 0.95\}$	$\{0.05, 0.1, \dots, 0.45, 0.5\}$	$\{0.5, 0.55, \dots, 0.9, 0.95\}$
$\check{\gamma}$	$\{0.05, 0.1, \dots, 0.9, 0.95\}$	$\{0.05, 0.1, \dots, 0.45, 0.5\}$	$\{0.5, 0.55, \dots, 0.9, 0.95\}$

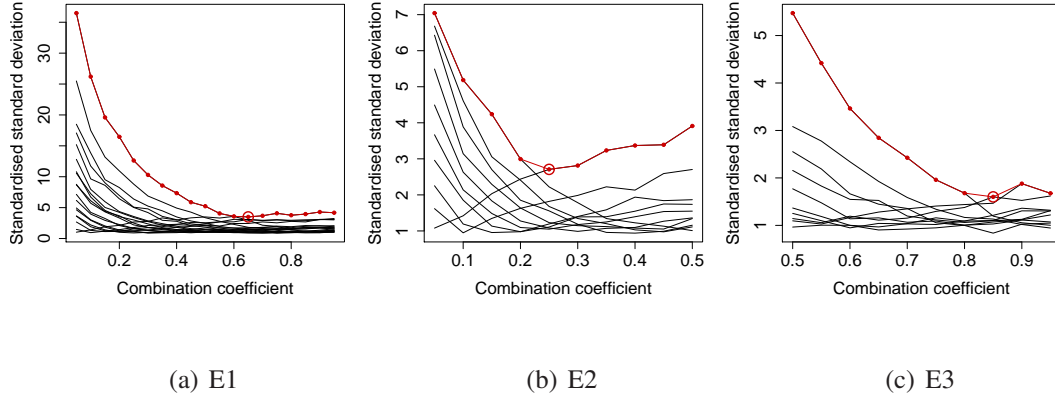


Figure 2. Results of the simulations in Series E: curves of SSD against $\check{\gamma}$.

$\gamma_i \in [0, 1]$, and $f_{P,i}$ and $f_{D,i}$ are the densities of population and cases in the i -th sub-square, respectively. Series R also contains three groups of simulations, R1 to R3. The settings are shown in Table 2, in which there are 20 independent settings for $\gamma_1, \dots, \gamma_4$ in each group, and the corresponding results are given in Figure 3. For example, in Group R1, each setting of f_I is obtained by generating $\gamma_1, \dots, \gamma_4 \stackrel{\text{i.i.d.}}{\sim} U[0.02, 0.98]$. Under each setting of f_I , $\check{\gamma}$ takes the 19 values in $\{0.05, 0.1, 0.15, \dots, 0.9, 0.95\}$ one by one, and the corresponding values of $\text{SSD}(\check{\gamma})$ are calculated, and they form a black curve in Figure 3(a). The robust setting of $\check{\gamma}$ is the one that minimises the maximum SSD, i.e., the one that minimises the red bold curve in Figure 3(a), which is marked out by a red circle. The three subfigures in Figure 3 seem more tanglesome than those in Figure 2, which is caused by the complex setting of f_I in Series R. However, the phenomenon presented in Figure 3 is similar to that in Figure 2, i.e., in each subfigure, the red

Table 2. Settings of f_1 and $\check{\gamma}$ in the simulations in Series R.

	Group R1	Group R2	Group R3
γ_i 's	[0.02, 0.98]	[0.02, 0.53]	[0.47, 0.98]
$\check{\gamma}$	{0.05, 0.1, \dots , 0.9, 0.95}	{0.05, 0.1, \dots , 0.45, 0.5}	{0.5, 0.55, \dots , 0.9, 0.95}

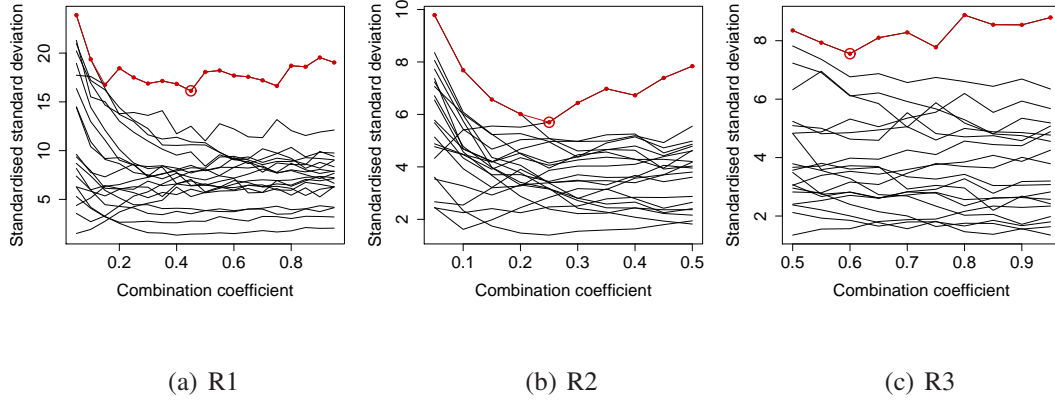


Figure 3. Results of the simulations in Series R: curves of SSD against $\check{\gamma}$.

bold curve becomes high when $\check{\gamma}$ is near the end of the domain of the γ_i 's, but becomes low when $\check{\gamma}$ is around the mid-point of that domain. It indicates again that the mid-point of the possible range of γ_i 's is a robust setting of $\check{\gamma}$. Some additional simulations in the Supplementary Material also present the similar phenomenon clearly. Therefore, according to the above simulations under different settings of γ , when a possible range of the value of γ is available, we should set $\check{\gamma}$ around the mid-point of that range, which is robust in the sense that the maximum value of SSD over all possible settings of f_1 would not be very large.

5.2. Comparisons

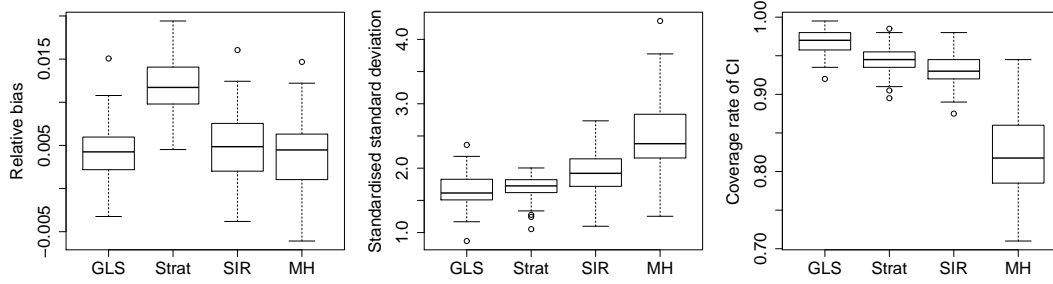
In this subsection, we show some comparisons for the GLS against other popular methods, including the SIR, MH and the stratified sampling. In this simulation, the region $\mathcal{R} = [0, 1]^2$

is divided into 16 equal-sized sub-squares (which is similar to the previous subsection) within each of which the density of the population is uniform, while the densities of the cases and infections are proportional to a normal distribution. In each of the 16 sub-squares, the population is fixed, but the numbers of cases and infections are generated randomly. Please refer to the Supplementary Material for more details about the settings. As for the sampling methods, we use the same sampling strategy in Algorithm 2, except for the sampler in Step 2. In our proposed method, the size of the uniform design used in the GLS $M = 210$. The proposal distributions in the SIR and MH samplers are set as the uniform distribution on $\mathcal{R} = [0, 1]^2$, and the normal distribution with covariance matrix equal to $1/16 \cdot \mathbf{I}_2$, respectively. In the three methods GLS, SIR and MH, the number of sampling positions $r = 16$, and the value of $\check{\gamma}$ is set 0 so that $\varphi \propto f_D$. In the stratified sampling, the strata are the 16 sub-squares and the Neyman allocation is used to determine the sample sizes in each stratum. The total population $N_P = 8000 \times 10^4$ and the total sample size $n = 1 \times 10^4$.

We use the following three criteria to compare their performances:

1. Relative bias: the ratio of the bias of \hat{N}_I to the true value of N_I ;
2. Standardised standard deviation: the ratio of the standard deviation of the estimator of N_I , obtained by a particular method, to that obtained by our method with the exact optimal settings, which is similar to that in Section 5.1;
3. Coverage rate of CI: the coverage rate of the approximate 95% CI.

We use 100 different random settings of f_I and f_D . Under each of the 100 settings, for each method, the values of these three criteria are calculated through 200 independent simulations. The results are presented in Figure 4. The unbiasedness of the estimators of N_I obtained by these



(a) Relative bias (b) Standardised standard deviation (c) Coverage rate of CI

Figure 4. Comparisons of different sampling methods.

four methods is verified through Figure 4(a). From Figure 4(b), we can find that our method has the smallest SSD, i.e., the minimum variance of the estimator of N_I . The main reasons are that the performance of the SIR sampler depends heavily on the quality of the initial samples from the proposal distribution, that the MH sampler is easy to get stuck at some peak of the density function, and that the stratified sampling method does not utilise the information about the population and the cases sufficiently. From Figure 4(c), we can also find that our method has the highest coverage rate of the approximate 95% CI of N_I . Therefore, we can conclude that our method is efficient, in the sense that its estimator of N_I is unbiased, with a small variance and a high coverage rate of the CI.

6. A Practical Example

To further illustrate the two-stage sampling strategy, an example based on the situation of COVID-19 in the USA is presented in this section. The ‘USA’ mentioned in this section refers to the 50 states of the USA, as well as the District of Columbia, excluding other territories of the USA. The cumulative numbers of diagnosed cases of the 51 administrative districts in the USA can be obtained from the Centers for Disease Control and Prevention (2020). Assume

that the true densities of population f_P , cases f_D and infections f_I are the densities of population, cases up to December 27th, 2020, and cases up to April 22nd, 2021 in the USA, respectively. The corresponding densities are depicted in Figure 5(a)–(c), with the unit being km^{-2} , and the specific data are shown in the Supplementary Material. The total population and the numbers of cases and infections are $N_P = 331.319 \times 10^6$, $N_D = 29.701 \times 10^6$ and $N_I = 31.467 \times 10^6$, respectively. The total sample size n is set as 10000, which is quite small compared to the total population of the USA. For comparison, we use both our method and the classical stratified sampling to estimate the total number of infections N_I . Based on the settings of N_P and N_D , it is reasonable to assume that the values of the true γ are in the range $[0, 0.1]$, and we set $\check{\gamma} = 0.05$ to obtain the initial rough estimation of f_I . In our method, we choose $r = 250$ and $M = 210$, as recommended in the previous sections, and the settings of the sampling density φ and the allocation method of the sample sizes are nearly optimal. As for the stratified sampling, the strata are defined as the 51 administrative districts, which is consistent with the area partition when recoding the epidemic-related data; the Neyman allocation (Lohr 2019) was used. The details about the stratified sampling are described in the Supplementary Material.

The results of 200 rounds of independent simulations are shown in Table 3. Though the standard deviation of the estimator obtained by our proposed method is slightly smaller than that of the stratified sampling, our method has higher coverage rate of CI. Note that in practice, the samples must be drawn from several selected sampling positions in each stratum. Due to this, the stratified multi-stage sampling is often used (Pollán et al. 2020), which can further increase the variance of the estimator. For the stratified multi-stage sampling method, big efforts have to be made in order to adapt to a complicated distribution of population, and the variance may become difficult to estimate. However, our method can automatically utilise the compli-

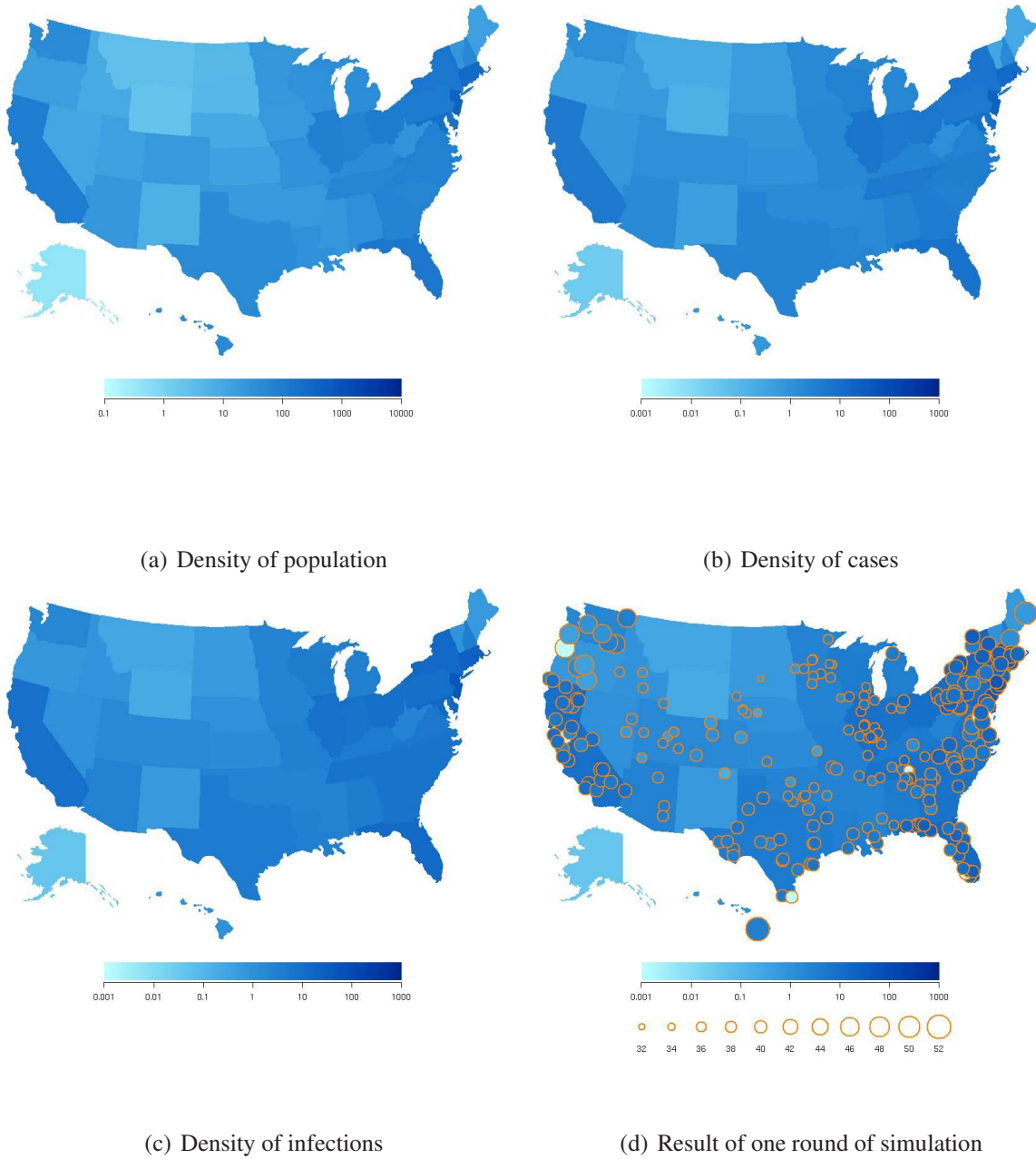


Figure 5. (a)–(c): The densities of population, cases and infections; (d): the result of one round of simulation.

cated information about the distributions of population and cases, while also maintaining the simplicity in estimating N_I and its variance.

Further, we show the result of one of the 200 rounds of simulations to explain our method. In this round of simulation, the estimated number of infections $\hat{N}_I = 29.70 \times 10^6$, with the

Table 3. Results of the comparison between our method and the stratified sampling.

Method	Sample mean of \hat{N}_I	Sample standard deviation of \hat{N}_I	Coverage rate of CI
Our method	31.612×10^6	0.995×10^6	99.5%
Stratified sampling	31.691×10^6	1.000×10^6	95.0%

estimated standard deviation $\sqrt{\hat{v}(\hat{N}_I)} = 1.36 \times 10^6$. The approximate 95% CI does cover the true N_I . The sampling positions are presented in Figure 5(d), where the background is the true f_I , and the circles represent the sampling positions, with their colours showing the estimated values of f_I in km^{-2} , and their diameters showing the sample sizes there. The final total sample size in this round is 9999, smaller by 1 than the expected $n = 10000$, due to the round-off error at each sampling position. The sample sizes at these sampling positions are nearly the same, which is determined by the characters of f_P and f_D , as well as $\check{\gamma}$.

7. Conclusions

In this paper, we propose a novel, two-stage sampling strategy to estimate the number of infections of a pandemic. Our method can sufficiently utilise the information about the distributions of both the population and the diagnosed cases, which can gather information more flexibly than the existing methods, and hence, more efficient. Moreover, our two-stage sampling strategy does not involve any discrete structures like strata or clusters, therefore, it can easily and automatically adapt to the complicated distributions of population and cases, and the corresponding estimating method keeps simple. The GLS algorithm used in our method is also easy to implement, since it does not need a proposal distribution. Its performance is robust against the complexity and multimodality of the sampling density, which overcomes the drawbacks of

the other popular samplers for general probability densities, such as the SIR or MH algorithm.

Since the true density of the infections is not known in practice, obtaining the exact optimal settings of the sampling density and the allocation function in this sampling strategy is unrealistic. Instead, we discuss the nearly optimal ones for practical implementation, which is based on an initial rough estimate of the density of infections. The total sample size can be determined by the pre-defined estimation precision. The small sample sizes at the sampling positions can be avoided by modifying the allocation of sample sizes based on a convex combination. In addition, in the second stage of our method, we just consider the simple random sampling method for simplicity. To further improve the efficiency and eliminate the selection bias, other sampling methods like the stratified sampling can be taken into account, with some slight modifications for the corresponding formulae in the second stage. Further, by the numerical simulations, we discuss the robust setting of the combination coefficient for the rough estimator of the density of infections in the minimax sense. We also compare the GLS algorithm with the SIR, MH and stratified sampling methods in terms of the relative bias, standard deviation and coverage rate of CI. It shows that the GLS algorithm has the smallest standard deviation and the highest coverage rate of the approximate 95% CI. Moreover, we apply our method to the investigation of COVID-19 in the USA. Our method shows good performance and has higher coverage rate of CI compared with the stratified sampling. Hence, these simulations and the practical example verify the efficiency of our proposed two-stage sampling method, whatever the sampling density is.

Acknowledgments

This work was supported by the National Natural Science Foundation of China under Grant Nos. 11871288, 11771220 and 12131001; and Natural Science Foundation of Tianjin under 19JCZDJC31100. The first two authors contributed equally to this work.

References

- Anand, S., Montez-Rath, M., Han, J., Bozeman, J., Kerschmann, R. et al. (2020), 'Prevalence of SARS-CoV-2 antibodies in a large nationwide sample of patients on dialysis in the USA: a cross-sectional study', *The Lancet* **396**(10259), 1335–1344.
- Centers for Disease Control and Prevention (2020), 'COVID data tracker', https://covid.cdc.gov/covid-data-tracker/#cases_totalcases.
- Cochran, W. G. (1977), *Sampling Techniques*, third edn, John Wiley & Sons.
- Hastings, W. K. (1970), 'Monte Carlo sampling methods using Markov chains and their applications', *Biometrika* **57**, 97–109.
- Havers, F. P., Reed, C., Lim, T. W., Montgomery, J. M., Klena, J. D. et al. (2020), 'Seroprevalence of antibodies to SARS-CoV-2 in six sites in the United States, March 23–May 3, 2020', *medRxiv* .
- Horton-French, K., Dunlop, E., Lucas, R. M., Pereira, G. and Black, L. J. (2021), 'Prevalence and predictors of vitamin D deficiency in a nationally representative sample of Australian adolescents and young adults', *European Journal of Clinical Nutrition* .

- Jia, L., Du, Y., Chu, L., Zhang, Z., Li, F. et al. (2020), 'Prevalence, risk factors, and management of dementia and mild cognitive impairment in adults aged 60 years or older in China: a cross-sectional study', *The Lancet Public Health* **5**(12), e661–e671.
- Kissler, S. M., Kishore, N., Prabhu, M., Goffman, D., Beilin, Y. et al. (2020), 'Reductions in commuting mobility correlate with geographic differences in SARS-CoV-2 prevalence in New York City', *Nature Communications* **11**(4674).
- Knudsen, A. K. S., Stene-Larsen, K., Gustavson, K., Hotopf, M., Kessler, R. C. et al. (2021), 'Prevalence of mental disorders, suicidal ideation and suicides in the general population before and during the COVID-19 pandemic in Norway: A population-based repeated cross-sectional analysis', *The Lancet Regional Health — Europe* **4**(100071).
- Leong, P.-Y., Huang, J.-Y., Chiou, J.-Y., Bai, Y.-C. and Wei, J. C.-C. (2021), 'The prevalence and incidence of systemic lupus erythematosus in Taiwan: a nationwide population-based study', *Scientific Reports* **11**(5631).
- Li, Y., Shan, Z. and Teng, W. (2021), 'Estimated change in prevalence of abnormal thyroid-stimulating hormone levels in China according to the application of the kit-recommended or NACB standard reference interval', *EClinicalMedicine* **32**(100723).
- Lohr, S. L. (2019), *Sampling: Design and Analysis*, second edn, CRC Press/Chapman & Hall/Taylor & Francis Group.
- Mulenga, L. B., Hines, J. Z., Fwoloshi, S., Chirwa, L., Siwingwa, M. et al. (2021), 'Prevalence of SARS-CoV-2 in six districts in Zambia in July, 2020: a cross-sectional cluster sample survey', *The Lancet Global Health* .

- Nagashima, S., Ko, K., Yamamoto, C., Bunthen, E., Ouoba, S. et al. (2021), ‘Prevalence of total hepatitis A antibody among 5 to 7 years old children and their mothers in Cambodia’, *Scientific Reports* **11**(4778).
- Ning, J. and Tao, H. (2018), ‘Randomized quasi-random sampling/importance resampling’, *Communications in Statistics - Simulation and Computation* .
- Parenteau, C. S., Lau, E. C., Campbell, I. C. and Courtney, A. (2021), ‘Prevalence of spine degeneration diagnosis by type, age, gender, and obesity using Medicare data’, *Scientific Reports* **11**(5389).
- Pérez, C. J., Martín, J., Rufo, M. J. and Rojano, C. (2005), ‘Quasi-random sampling importance resampling’, *Communications in Statistics - Simulation and Computation* **34**(1), 97–112.
- Pollán, M., Pérez-Gómez, B., Pastor-Barriuso, R., Oteo, J., Hernán, M. A. et al. (2020), ‘Prevalence of SARS-CoV-2 in Spain (ENE-COVID): a nationwide, population-based seroepidemiological study’, *The Lancet* **397**(10250), 535–544.
- Rosenberg, E. S., Tesoriero, J. M., Rosenthal, E. M., Chung, R., Barranco, M. A. et al. (2020), ‘Cumulative incidence and diagnosis of SARS-CoV-2 infection in New York’, *Annals of Epidemiology* **48**, 23–29.
- Rubin, D. B. (1987), ‘A noniterative sampling/importance resampling alternative to the data augmentation algorithm for creating a few imputations when fractions of missing information are modest: the SIR algorithm’, *Journal of the American Statistical Association* **82**, 543–546.
- Sakurai, A., Sasaki, T., Kato, S., Hayashi, M., Tsuzuki, S.-i. et al. (2020), ‘Natural history of asymptomatic SARS-CoV-2 infection’, *New England Journal of Medicine* **383**(9), 885–886.

- Sartorius, B., Cano, J., Simpson, H., Tusting, L. S., Marczak, L. B. et al. (2021), ‘Prevalence and intensity of soil-transmitted helminth infections of children in sub-Saharan Africa, 2000-18: a geospatial analysis’, *The Lancet Global Health* **9**(1), e52–e60.
- Sood, N., Simon, P., Ebner, P., Eichner, D., Reynolds, J. et al. (2020), ‘Seroprevalence of sars-cov-2-specific antibodies among adults in Los Angeles County, California, on April 10–11, 2020’, *JAMA* **323**(23), 2425–2427.
- Ssentongo, P., Ssentongo, A. E., Ba, D. M., Ericson, J. E., Na, M. et al. (2021), ‘Global, regional and national epidemiology and prevalence of child stunting, wasting and underweight in low- and middle-income countries, 2006-2018’, *Scientific Reports* **11**(5204).
- Stringhini, S., Wisniak, A., Piumatti, G., Azman, A. S., Lauer, S. A. et al. (2020), ‘Seroprevalence of anti-SARS-CoV-2 IgG antibodies in Geneva, Switzerland (SEROCoV-POP): a population-based study’, *The Lancet* **396**(10247), 313–319.
- Tian, H., Hu, Y., Li, Q., Lei, L., Liu, Z. et al. (2021), ‘Estimating cancer survival and prevalence with the Medical-Insurance-System-based Cancer Surveillance System (MIS-CASS): An empirical study in China’, *EClinicalMedicine* **33**(100756).
- Wang, Y. J., Ning, J.-H., Zhou, Y.-D. and Fang, K.-T. (2015), A new sampler: randomized likelihood sampling, in ‘Souvenir Booklet of the 24th International Workshop on Matrices and Statistics’, pp. 255–261.
- Ward, H., Atchison, C., Whitaker, M., Ainslie, K. E. C., Elliott, J. et al. (2021), ‘SARS-CoV-2 antibody prevalence in England following the first peak of the pandemic’, *Nature Communications* **12**(905).

WHO (2020), 'Who director general's opening remarks at the media briefing on covid-19, <https://www.who.int/dg/speeches/detail/who-director-general-s-openingremarks-at-the-media-briefing-on-covid-19%2d%2d-11-march-2020>'.

Xu, X., Sun, J., Nie, S., Li, H., Kong, Y. et al. (2020), 'Seroprevalence of immunoglobulin M and G antibodies against SARS-CoV-2 in China', *Nature Medicine* **26**, 1193–1195.

Zhou, Y.-D., He, P., Ning, J.-H. and Fang, K.-T. (2021), *Methods and Applications of Stochastic Simulations*, Higher Education Press.